Shattering Transitions in Collision-Induced Fragmentation

P. L. Krapivsky*
Center for Polymer Studies and Department of Physics, Boston University, Boston, MA 02215

E. Ben-Naim†
Theoretical Division and Center for Nonlinear Studies,
Los Alamos National Laboratory, Los Alamos, NM 87545

We investigate the kinetics of nonlinear collision-induced fragmentation. We obtain the fragment mass distribution analytically by utilizing its travelling wave behavior. The system undergoes a shattering transition in which a finite fraction of the mass is lost to infinitesimal fragments (dust). The nature of the shattering transition depends on the fragmentation process. When the larger of the two colliding fragments splits, the transition is discontinuous and the entire mass is transformed into dust at the transition point. When the smaller fragment splits, the transition is continuous with the dust gaining mass steadily on the account of the fragments. At the transition point, the fragment mass distribution diverges algebraically for small masses, $c(m) \sim m^{-\alpha}$, with $\alpha = 1.20191\ldots$

PACS numbers: 05.40.-a, 05.20.Dd, 64.60.-i, 5.45.-a

I. INTRODUCTION

Fragmentation occurs in numerous physical phenomena and industrial processes [1–5]. Examples include breakup of liquid droplets [6] and atomic nuclei [7], polymer degradation [8], shattering of solid objects [9, 10], meteor impacts, and mineral grinding. Idealized models of such physical phenomena are also useful conceptual tools for describing complex systems such as fluid turbulence, spin glasses [11], genetic populations [12, 13], and random Boolean networks [14, 15].

In some cases, for example in polymer degradation, the evolution of a fragment depends only on its size. Therefore, fragments do not interact and such processes are inherently *linear*. In other cases including grinding processes, explosions in an enclosed volume, and breakup of eddies in a turbulent flow [16], interactions between fragments are essential. Such fragmentation processes are intrinsically *nonlinear* [17–20]. In this study, we show that the nature of the mass distribution changes qualitatively due to nonlinearities.

We investigate a basic class of nonlinear fragmentation processes where binary collisions are the cause of breakage. We show that such processes exhibit a shattering transition where infinitesimal fragments (dust) carry a finite fraction of the mass in the system. We consider the simplest realization where one of the two colliding fragments breaks into two pieces. Generically, the number of fragments diverges in a finite time, indicating shattering into dust.

The nature of the shattering transition depends sensitively upon the details of the fragmentation process, in particular, which of the two colliding particles splits. We investigate three possibilities: (A) either, (B) the larger, and (C) the smaller of the two particles breaks into two fragments upon collision. In the first two models, as the transition occurs the entire mass is instantly transformed into dust. In the third model, the dust mass gradually increases once the shattering transition occurred.

In contrast with linear fragmentation processes, explicit solutions of the nonlinear and non-local rate equations are generally not possible. Nevertheless, the most important physical characteristics can still be obtained analytically. Interestingly, the fragment mass distribution attains a travelling wave form as the transition is approached. Of the spectrum of possible propagation velocities, the extremal one is selected and it characterizes typical and extremal behaviors of the mass distribution. In the case of model C, at the shattering transition, the mass distribution is algebraic for small masses, with a transcendental exponent. Past the transition, the fragment mass distribution approaches a universal form.

We first consider the number density that manifests the shattering transition (section II). Then, we analyze the fragment mass distribution using rate equations for a deterministic version (section III) and a stochastic version (section IV) of the fragmentation process. Finally, we summarize our results and outline a few suggestions for future work (section V).

II. THE NUMBER DENSITY

Consider a fragmentation process where at each (binary) collision event, one particle splits into two pieces while the second particle remains intact. We restrict our attention to situations where the splitting rate is independent of the fragment size and without loss of generality, the collision rate is set to unity. Analogous to the kinetic theory description of collisions in molecular gases, we assume perfect mixing, namely, absence of spatial correlations between fragments. The total fragment density,

*Electronic address: paulk@bu.edu
†Electronic address: ebn@lanl.gov

$N(t)$, evolves according to the rate equation

$$\frac{d}{dt}\,N(t) = N^2(t). \qquad (1)$$

Without loss of generality, the initial density is set to unity, $N(0) = 1$, and therefore, the total density is

$$N(t) = \frac{1}{1-t}. \qquad (2)$$

In a finite time, the number of fragments diverges and the average fragment mass vanishes. This divergence indicates that the system undergoes a shattering transition at $t_c = 1$.

Let $\tau = \int_0^t dt'\,N(t')$ be the average number of collisions experienced by a fragment up to time t. This quantity diverges logarithmically

$$\tau = \ln N(t) = \ln\frac{1}{1-t}. \qquad (3)$$

This "collision counter" provides a convenient alternative measure of time.

III. DETERMINISTIC FRAGMENTATION

To complete the model definition we have to specify which of the fragments splits, and how it splits. Following Cheng and Redner [18], we consider three possibilities: (A) a randomly chosen, (B) the larger, and (C) the smaller fragment splits upon collision. In this section, we consider a deterministic rule where fragments split into two equal pieces. In the next section, we show that stochastic rules result in qualitatively similar behaviors.

A. Random particle splits

We start with the case where a randomly selected particle splits upon collision (this is equivalent to having both particles split). For simplicity, we focus on monodisperse initial conditions where all particles have unit mass, $m = 1$. Then, a fragment produced by n collision events has mass $m = 2^{-n}$. Let $c_n(t)$ be the density of such fragments at time t. This density evolves according to

$$\frac{d}{dt}\,c_n(t) = N(t)\,[\,2c_{n-1}(t) - c_n(t)\,], \qquad (4)$$

with the total density $N(t) = \sum_{j=0}^{\infty} c_j(t)$. Summing up Eqs. (4) we indeed recover Eq. (1). Also, the total mass, $M(t) = \sum_{j=0}^{\infty} 2^{-j}\,c_j(t)$, is conserved, $M(t) = 1$.

In terms of the collision counter, the process is linear, $\frac{d}{d\tau}\,c_n = 2c_{n-1} - c_n$, and subject to the monodisperse initial conditions $c_n(0) = \delta_{n,0}$, the exact solution is the Poissonian density [18]

$$c_n(\tau) = e^{-\tau}\,\frac{(2\tau)^n}{n!}\,. \qquad (5)$$

At the shattering time $t_c = 1$ (corresponding to $\tau = \infty$), the densities vanish: $c_n(t = 1) = 0$ for all n. Therefore, the fragment mass density undergoes a first-order (discontinuous) transition, $M(t) = \Theta(t_c - t)$ with Θ the Heaviside step function. In other words, the entire mass is shattered into dust and there are no particles with positive mass [8, 18, 21].

Near the shattering transition, *i.e.*, as $\tau \to \infty$, the mass distribution approaches

$$c_n(\tau) \to \frac{N}{\sqrt{v\tau}}\,G\left(\frac{n - v\tau}{\sqrt{v\tau}}\right)\,, \qquad (6)$$

where $v = 2$ and $G(x) = (2\pi)^{-1/2}\exp\left(-x^2/2\right)$ is the Gaussian distribution. Since $n = \log_2(1/m)$, the mass distribution becomes log-normal, a behavior typical to fragmentation and cascade processes [2, 8, 18, 21].

B. Larger particle splits

Now in a collision the larger particle splits into two equal pieces. If the colliding particles have the same mass, a randomly chosen particle splits. The fragment mass density, $c_n \equiv c_n(t)$, satisfies the rate equation

$$\frac{d}{dt}\,c_n = 4c_{n-1}A_n - 2c_nA_{n+1} + 2c_{n-1}^2 - c_n^2\,, \qquad (7)$$

where A_n is the cumulative density of fragments of mass 2^{-n} and smaller, $A_n(t) = \sum_{j=n}^{\infty} c_j(t)$. The initial conditions are $c_n(0) = \delta_{n,0}$. One can verify that the mass is conserved, $M(t) = 1$, and that the total density is given by Eq. (2).

The density $c_0(t)$ of unit mass particles satisfies the Bernoulli equation, $\frac{d}{dt}\,c_0 = c_0^2 - 2c_0N$. Using Eq. (2) and the initial condition $c_0(0) = 1$ gives

$$c_0(t) = \frac{3(1-t)^2}{2 + (1-t)^3}\,. \qquad (8)$$

For sufficiently small n, one can obtain the leading asymptotic behavior near the shattering transition. Since $A_n \to N$ as $t \to 1$ and the last two terms on the right-hand side of Eq. (7) are asymptotically negligible, the rate equations simplify to $\frac{d}{dt}\,c_n = 2N(2c_{n-1} - c_n)$ which are identical (up to the factor 2) to Eqs. (4). Therefore,

$$c_n(\tau) \propto e^{-2\tau}\,\frac{(4\tau)^n}{n!}. \qquad (9)$$

Apart from logarithmic corrections, the densities vanish quadratically: $c_n(t) \propto (1-t)^2$. We conclude that the shattering transition remains discontinuous (see Fig. 1). Figure 1 suggests studying the normalized distribution $N^{-1}c_n(t)$. Below, we show that as a function of τ, the normalized fragment mass distribution follows a universal behavior in the large-n limit.

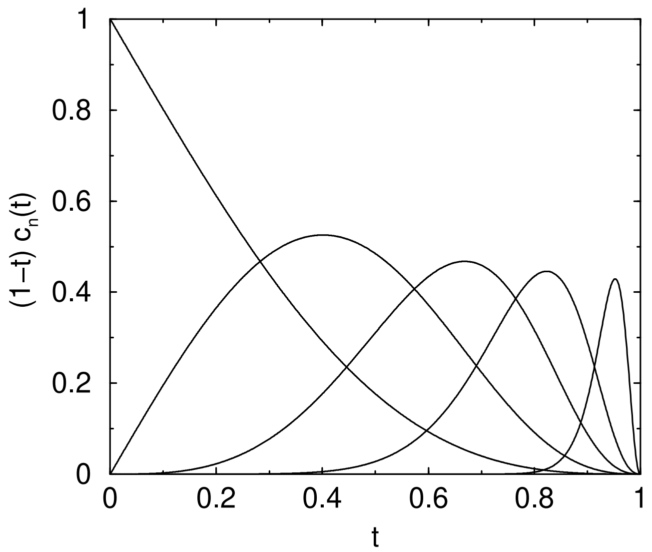

FIG. 1: The normalized fragment size distribution. Shown is $N^{-1}c_n(t)$ versus t for $n = 0$, 1, 2, 4, and 6. The numerical results reported in this study were obtained from integration of the rate equations using the Adams-Bashford method with an adaptive time step yielding a relative accuracy of 10^{-9} in the densities.

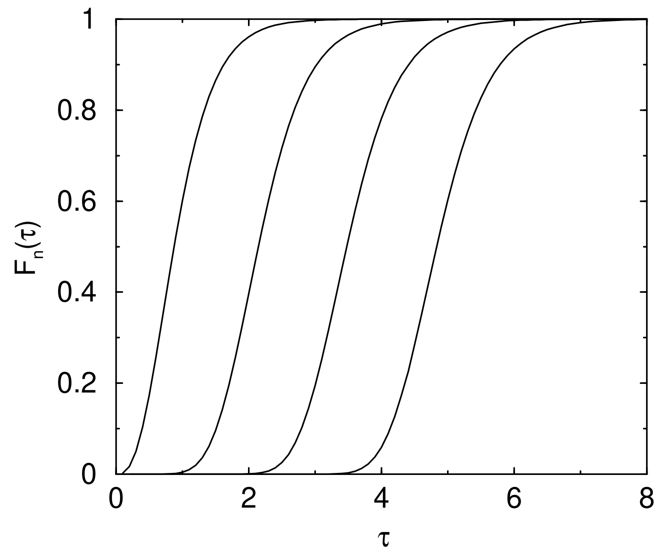

FIG. 2: The travelling wave. Shown are numerical solutions of Eq. (11) for $n = 2$, 4, 6, and 8.

The rate equations (7) simplify in terms of the cumulative densities:

$$\frac{d}{dt}\,A_n = 2A_{n-1}^2 - A_n^2\,. \tag{10}$$

This equation holds for $A_0 = N$ if we set $A_{-1} \equiv A_0$. The initial conditions are $A_n(0) = \delta_{n,0}$. We characterize time by the collision counter (3) and normalize the size density by the total number density, $F_n(\tau) = N^{-1}A_n(t)$. These transformations yield

$$\frac{d}{d\tau}\,F_n = 2F_{n-1}^2 - F_n^2 - F_n\,. \tag{11}$$

Asymptotically, this equation admits a travelling wave solution $F_n(\tau) \to f(n - v\tau)$ as shown in Fig. 2. The wave form $f(x)$ satisfies the difference-differential equation

$$v\frac{d}{dx}f(x) = f(x) + f^2(x) - 2f^2(x-1)\,, \tag{12}$$

and is subject to the boundary conditions $f(-\infty) = 1$ and $f(\infty) = 0$. Remarkably, the velocity v can be determined without solving the nonlinear and non-local differential equation (12) exactly. It follows from the exponential behavior attained by $f(x)$ far behind the front: $1 - f(x) \sim e^{\lambda x}$ as $x \to -\infty$. Together with Eq. (12) it yields a "dispersion" relation between the velocity v and the decay coefficient λ,

$$v = \frac{3 - 4e^{-\lambda}}{\lambda}\,. \tag{13}$$

Out of the spectra of possible velocities $v \in (-\infty, v_{\max}]$, the maximal value is selected. At the maximum, we have $3e^{\lambda} = 4(1+\lambda)$, from which $\lambda \cong 0.961279$ and $v \cong 1.52961$. Alternatively, the velocity is the smaller root of $v\ln(4e/v) = 3$.

Velocity selection underlies numerous situations, yet it has been rigorously established only for a few non-linear parabolic partial differential equations, typically occurring in reaction-diffusion problems [22–27]. Recently, velocity selection has been also applied to a host of difference and difference-differential equations [28–32] including a linear fragmentation process [30]. Typically, the selected velocity gives key physical characteristics such as the growth velocity of a surface in deposition processes [28] or the extremal heights of random trees [32].

The typical behavior of the fragment mass density follows from the travelling wave form

$$c_n(\tau) \to N\,g(n - v\tau)\,, \tag{14}$$

with $g(x) = f(x) - f(x+1)$. The front location $n_* \approx v\tau$ characterizes typical fragments and the typical mass $m_* = 2^{-n_*}$ shrinks as

$$m_* \sim (1-t)^{\sigma} \tag{15}$$

with $\sigma = v\ln 2 \cong 1.06024$ as $t \to 1$. The typical mass decays slower than in model A where $\sigma = 2\ln 2 \cong 1.38629$. Another difference between models A and B is manifested by the width: In contrast with the diffusive broadening in model A the width saturates at a finite value in model B. Yet, fundamentally the shattering transitions are the same in both models — the entire system is instantly transformed into dust at the transition point.

The extremal behavior of the fragment mass density follows from the tails of $f(x)$. The behavior far ahead of the wave front ($x \to \infty$) is a sharp double exponential decay, as implied by the leading terms in Eq. (12),

$v\frac{d}{dx}f(x) = -2f^2(x-1)$. In summary, the extremal behaviors are

$$f(x) \sim \begin{cases} 1 - C_1\, e^{\lambda x} & x \to -\infty, \\ 2^x\, \exp(-C_2\, 2^x) & x \to +\infty. \end{cases} \quad (16)$$

We now re-express the mass distribution in terms of the ordinary mass variable $m = 2^{-n}$. The two distributions are related via $c(m)dm = c_n dn$ (note that large masses correspond to small indices and vice versa). Near the shattering transition, the mass distribution attains the scaling form $c(m) \to \frac{N}{m_*}\mathcal{F}\left(\frac{m}{m_*}\right)$. Equation (16) leads to the following extremal behaviors of the scaling function:

$$\mathcal{F}(z) \sim \begin{cases} z^{-\alpha} & z \gg 1, \\ z^{-2}\exp\left(-C_2\, z^{-1}\right) & z \ll 1; \end{cases} \quad (17)$$

with $\alpha = 1 + \lambda/\ln 2 \cong 2.38683$. Hence, large masses (relative to the typical mass) are suppressed algebraically, while small masses are suppressed exponentially.

Generally, in fragmentation processes the mass distribution has a scaling form and this is indeed the case for collision-induced fragmentation. However, the nonlinear nature of the process results in qualitative changes to the scaling behavior. The similarity solutions have two scales characterizing the front location and fluctuations around it in the linear case (model A). In contrast, only a single scale underlies similarity solutions in the nonlinear case (model B).

C. Smaller particle splits

When the smaller particle splits upon collision the fragment size densities satisfy the rate equations

$$\frac{d}{dt}c_n = 4c_{n-1}B_{n-1} - 2c_nB_n + 2c_{n-1}^2 - c_n^2\,, \quad (18)$$

where $B_n = \sum_{j=0}^{n-1} c_j$ is the cumulative density of particles with mass larger than 2^{-n}.

The density of unit mass particles is readily found by solving $\dot{c}_0 = -c_0^2$. The next density can be found as well

$$\begin{aligned} c_0(t) &= \frac{1}{1+t}\,, \\ c_1(t) &= \frac{2}{1+t}\,\frac{(1+t)^3-1}{2(1+t)^3+1}\,. \end{aligned} \quad (19)$$

These explicit results already demonstrate that densities are *positive* at all times. Hence, the total mass density $M(t)$ also remains positive after the shattering transition.

The kinetics just below and at the shattering transition can be determined using the travelling wave behavior. The cumulative distribution obeys $\frac{d}{dt}B_n = 2B_{n-1}^2 - B_n^2$ which is identical to Eq. (10); the initial conditions, however, are different: $B_n(0) = 1 - \delta_{n,0}$. The transformed distribution $F_n(\tau) = N^{-1}B_n$ again evolves according to

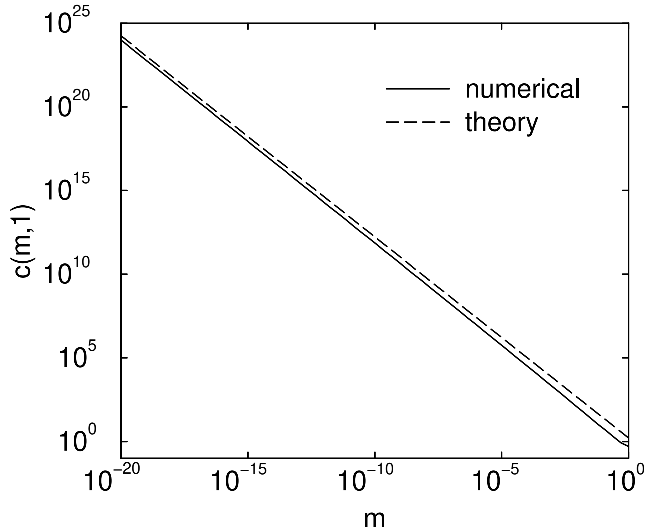

FIG. 3: The mass distribution at the shattering time. Numerical integration of the rate equations (18) are compared with the theoretical prediction (23).

Eq. (11). Asymptotically, it admits a travelling wave solution, $F_n(\tau) \to f(n - v\tau)$, with the wave form $f(x)$ satisfying Eq. (12). However, the boundary conditions are reversed, $F(-\infty) = 0$ and $F(\infty) = 1$, leading to different quantitative and qualitative results.

Both extremal behaviors are now exponential

$$f(x) \sim \begin{cases} e^{x/v} & x \to -\infty, \\ 1 - e^{-\lambda x} & x \to +\infty. \end{cases} \quad (20)$$

The behavior far ahead of the front is used to determine the velocity. The dispersion relation is

$$v = \frac{4e^\lambda - 3}{\lambda}\,, \quad (21)$$

and the extremum selection principle gives $\lambda \cong 0.58013$ and $v \cong 7.14509$. Numerically, we confirmed this velocity to within 0.01%. Interestingly, v is the larger root of the same (as in model B) equation $v\ln(4e/v) = 3$. We note that the velocities satisfy $v_B < v_A < v_C$.

The fragment size distribution follows the travelling wave form (14) with $g(x) = f(x+1) - f(x)$. The typical mass shrinks according to (15) with $\sigma = v\ln 2 \cong 4.9526$ near the shattering point. The exponential tails of the wave form imply algebraic tails for the scaling function underlying the mass distribution

$$\mathcal{F}(z) \sim \begin{cases} z^{-\alpha} & z \gg 1, \\ z^{-\beta} & z \ll 1; \end{cases} \quad (22)$$

with $\alpha = 1 + (v\ln 2)^{-1} \cong 1.20191$ and $\beta = 1 - \lambda/\ln 2 \cong 0.163049$.

Our major result is that the mass distribution diverges algebraically at the transition time [33]:

$$c(m,1) \sim m^{-\alpha}, \quad (23)$$

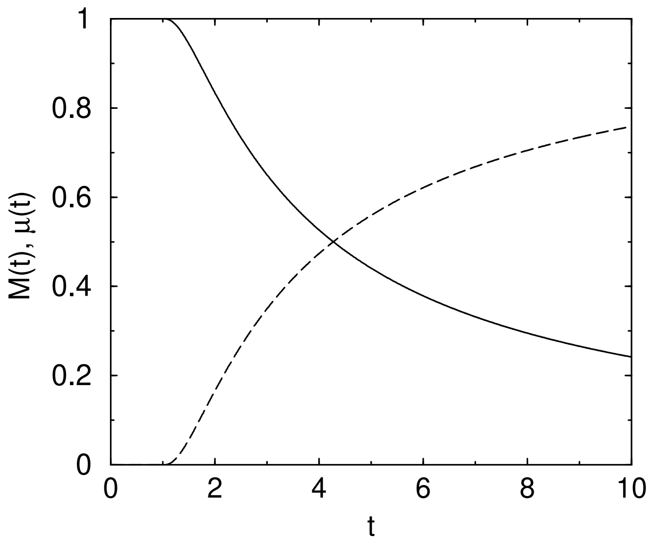

FIG. 4: Fragment versus dust mass. Shown are the fragment mass $M(t)$ (solid line) and the dust mass $\mu(t)$ (dashed line) versus time t.

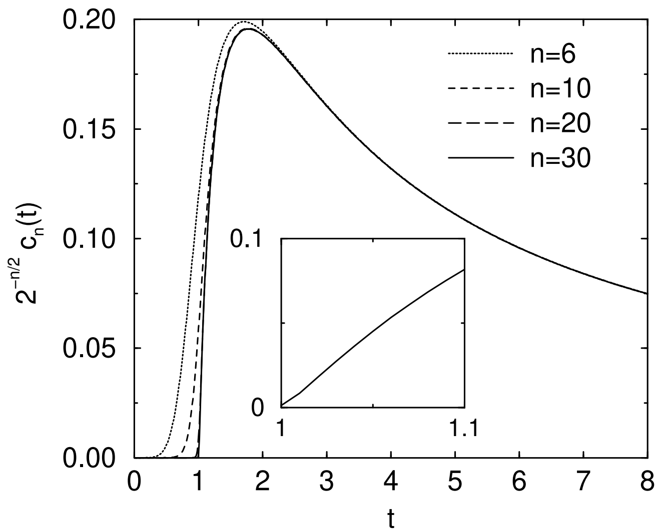

FIG. 5: The asymptotic behavior of the size density. Shown is $2^{-n/2}c_n(t)$ versus t for $n = 6$, 10, 20, and 30. The inset shows the behavior in the vicinity of $t = 1$ for $n = 30$ (axis labels are as in the main figure).

for $m \to 0$ with the transcendental exponent $\alpha = 1.20191$ (Fig. 3). This behavior can be obtained from the large-z behavior of $\mathcal{F}(z)$. Although in general the travelling wave form implies time-dependent densities, when $z \to \infty$, the mass densities become *stationary.*

Model C exhibits a rich post-transition behavior. The explicit solutions (19) suggest that $c_n \simeq \gamma_n\, t^{-1}$ when $t \to \infty$. Indeed, this behavior is compatible with Eqs. (18) and the cumulative amplitudes $\Gamma_n = \sum_{j=0}^{n} \gamma_j$ satisfy the recursion relation $\Gamma_n^2 - \Gamma_n = 2\Gamma_{n-1}^2$ with $\Gamma_0 = 1$. The amplitudes grow exponentially, $\gamma_n \sim \Gamma_n \sim 2^{n/2}$. Summing over densities, the total fragment mass decays as

$$M(t) \simeq C\, t^{-1} \quad \text{as} \quad t \to \infty, \tag{24}$$

with $C = \sum_{n=0}^{\infty} 2^{-n}\gamma_n \cong 2.66084$. Thus, the total fragment mass remains positive at all times. The dust mass, $\mu(t) = 1 - M(t)$, vanishes at the shattering time, $\mu(1) = 0$, and it gradually increases for $t > 1$ (Fig. 4). Only in the long time limit it accounts for the entire mass in the system. We conclude that in model C, the shattering transition is continuous.

Numerically, we observe that for sufficiently large n, the densities follow a universal behavior (Fig. 5)

$$c_n(t) \to 2^{n/2}\, u(t). \tag{25}$$

While this ansatz is asymptotic with respect to n, it holds for *all* times. The function $u(t)$ vanishes below the shattering time and grows linearly afterwords, $u(t) \sim (t-1)$ for $t - 1 \to 0$. Hence, this function plays the role of an order parameter. Note also that $u(t) \sim t^{-1}$ as $t \to \infty$.

The order parameter and the total dust mass are intimately related. Consider the total mass density of fragments of mass 2^{-k} or larger: $M^{(k)}(t) = \sum_{n=0}^{k} 2^{-n}\, c_n(t)$. From the rate equations (18), this mass density decreases according to

$$\frac{d}{dt}\, M^{(k)}(t) = -2^{-k} c_k \left(2B_k + c_k\right). \tag{26}$$

The flux of mass from fragments into dust is simply $\frac{d}{dt}\,\mu = -\lim_{k\to\infty} \frac{d}{dt}\, M^{(k)}$. Using Eq. (25), the right-hand side of Eq. (26) approaches $\left(3 + 2\sqrt{2}\,\right) u^2(t)$ in the limit $k \to \infty$ and therefore,

$$\frac{d}{dt}\,\mu(t) = \left(3 + 2\sqrt{2}\right) u^2(t). \tag{27}$$

This in turn shows that the dust mass grows according to $\mu(t) \sim (t-1)^3$ past the transition.

IV. STOCHASTIC FRAGMENTATION

We now briefly describe a generalized collision-induced fragmentation process where splitting is stochastic. Specifically, a particle of mass m splits into two fragments of mass m' and $m - m'$ with m' chosen stochastically from the interval $0 < m' < m$ according to some fixed distribution. We focus on the simplest case of uniform splitting, i.e., m' is chosen uniformly in $[0, m]$.

A. Model A

When a randomly selected particle splits, the mass density $c(m, \tau)$ satisfies

$$\frac{\partial}{\partial \tau}\, c(m,\tau) = -c(m,\tau) + 2\int_m^\infty \frac{dm'}{m'}\, c(m',\tau). \tag{28}$$

The kernel $1/m'$ reflects the uniform splitting probability and the collision rate N is absorbed by the collision counter τ. This equation is solved using the Mellin transform and for the monodisperse initial condition, $c(m,0) = \delta(m-1)$, one finds [34]

$$c(m,\tau) = e^{-\tau}\delta(m-1) + e^{-\tau}\sqrt{\frac{2\tau}{\ln\frac{1}{m}}}\; I_1\left[\sqrt{8\tau\ln\frac{1}{m}}\right]$$

with I_1 the modified Bessel function. The first term on the right-hand side simply describes the density of particles that have yet to collide. The second term simplifies asymptotically. Making the transformation $m = e^{-n}$ leads to a normal distribution as in (6) with the propagation velocity $v = \frac{32}{9}$.

B. Model B

When the larger of the two fragments splits, the rate equations for the mass density $c(m) \equiv c(m,\tau)$ are

$$\frac{\partial}{\partial t}c(m) = 4\int_m^\infty \frac{dm'}{m'}c(m')A(m') - 2c(m)A(m)\,, \quad (29)$$

with the cumulative density $A(m) = \int_0^m dm' c(m')$. We employ the same transformations used in the deterministic case. Characterizing the mass m by "index" n via $m = e^{-n}$, the fragment size density, $c(n)$, evolves according to

$$\frac{\partial}{\partial t}\,c(n) = 4\int_0^n dn' e^{n'-n}c(n')A(n') - 2c(n)A(n) \quad (30)$$

with $A(n) = \int_n^\infty dn' c(n')$. This cumulative distribution satisfies

$$\frac{\partial}{\partial t}\,A(n) = A^2(n) - 2\int_0^n dn'\, e^{n'-n}\frac{\partial}{\partial n'}A^2(n')\,. \quad (31)$$

Expressing time in units of the collision counter and normalizing by the total density, $F(n,\tau) = N^{-1}A(n)$, we transform Eq. (31) into

$$\frac{\partial}{\partial \tau}\,F(n) = F^2(n) - F(n) - 2\int_0^n dn'\, e^{n'-n}\frac{\partial}{\partial n'}F^2(n')\,.$$

Seeking a travelling wave solution $F(n,\tau) \to f(n - v\tau)$ yields the non-linear integro-differential equation

$$v\frac{d}{dx}f(x) = f(x) - f^2(x) + 2\int_{-\infty}^x dy\, e^{y-x}\frac{d}{dy}f^2(y)\,, \quad (32)$$

subject to the boundary conditions $f(-\infty) = 0$ and $f(\infty) = 1$. The exponential decay $1 - f(x) \sim \exp(\lambda x)$ as $x \to \infty$ gives the dispersion relation $v = 4(1+\lambda)^{-1} - \lambda^{-1}$ and the extremum selection principle yields $\lambda = v = 1$. Close to the shattering transition, the typical mass is proportional to the average mass, $m_* \sim (1-t)$ [35]. The mass densities behave as in the deterministic case and the extremal behaviors (17) are recovered with $\alpha = 2$. The nature of the transition is discontinuous, as in the deterministic case.

C. Model C

When the smaller particle splits upon collision, the rate equations for the mass density are

$$\frac{\partial}{\partial t}c(m) = 4\int_m^\infty \frac{dm'}{m'}\; c(m')B(m') - 2c(m')B(m') \quad (33)$$

with $B(m,t) = \int_m^\infty dm'\, c(m',t)$. In terms of the index n, the cumulative density $B(n,t) = \int_0^n dn' c(n')$ obeys Eq. (31). The normalized cumulative density again admits the travelling wave form. The velocity and decay rate are $v = 9$ and $\lambda = \frac{1}{3}$. At the shattering time, the (finite) mass distribution diverges algebraically: $c(m,1) \sim m^{-\alpha}$ with $\alpha = 10/9$. Past the shattering transition, the asymptotic ansatz $c(m,t) \to m^{-3/2}\,u(t)$ holds for small masses and the dust mass is related to the order parameter via $\frac{d}{dt}\mu = 2u^2$. We conclude that qualitatively, the shattering transition is similar to the deterministic case.

V. DISCUSSION

We investigated kinetic properties of collision-induced fragmentation processes. Generally, the mass is transferred from finite fragments into infinitesimal dust in a finite time. The nature of the shattering transition depends on the fragmentation process. When the larger of the colliding particles splits or when a randomly selected one splits, the transition is discontinuous and the entire mass is transformed into dust instantaneously. When the smaller particle splits, the transition is continuous, with the dust accumulating gradually past the shattering transition. In this case, finite fragments always carry a non-zero fraction of the mass.

Model A is essentially linear and thus solvable. For models B and C the nonlinear and non-local governing equations can not be solved in a closed form. Nevertheless, in the vicinity of the shattering transition we were able to obtain the most important characteristics analytically by utilizing the traveling wave form of the fragment mass density. The mass distribution follows a scaling behavior with a single characteristic scale, in contrast with the two scales found for linear processes.

For model C, the post-shattering behavior is nontrivial. At the transition point, the mass distribution decays algebraically, $c(m) \sim m^{-\alpha}$, with a transcendental exponent $\alpha = 1.20191\ldots$ in deterministic fragmentation and a rational exponent $\alpha = 10/9$ in stochastic fragmentation. We have also demonstrated that the mass densities exhibit universal asymptotic behavior (25) in the post-shattering region.

A challenging open problem is the complete post-shattering behavior in model C, for example, the time dependent dust mass. This is largely a mathematical problem since physically, the breakage of sufficiently small fragments is impossible. For instance, micro-cracks on the surface of the fragment are often precursors for breakage. The number of such surface defects is proportional to the surface area, so sufficiently small fragments are effectively unbreakable.

We focused on the leading asymptotic behavior. There are however corrections to the linear front propagation [24–27]. The traveling wave solution is actually a function of $x = n - X(\tau)$ with the position of the front $X(\tau)$ given by $X(\tau) = v\tau \pm \frac{3}{2\lambda}\ln\tau + \mathcal{O}(1)$. The plus and minus signs correspond to model B and C, respectively. This translates to a logarithmic correction to the typical mass (15).

We treated the problem using a mean-field rate equation approach. Thus we ignored correlations between the colliding particles. In principle, spatial correlations may be important up to some critical dimension beyond which they can indeed be ignored. The analysis of this possibility requires a more complete description of the process. Particularly, one must specify the transport mechanism.

Collision-induced fragmentation arises most naturally in processes where particles moves ballistically between collisions. Using dimensional analysis we argue that the shattering transition always occur in ballistic fragmentation. The typical mean free time T, velocity v, particle cross section s, and number density N are related via $NvTs \sim 1$. Mass conservation implies $m \sim N^{-1}$ (here m is the typical mass), while energy conservation gives $v \sim 1$. Finally $m \sim s^{d/(d-1)}$ yields $s \sim N^{-1+1/d}$. In particular, $T \sim N^{-1/d}$. The particle density evolves according to $\frac{d}{dt}N = N/T$, or $\frac{d}{dt}N \sim N^{1+1/d}$ from which $N \sim (t_c - t)^{-d}$. Based on this heuristic argument, we speculate that in ballistic fragmentation, the shattering transition occurs in arbitrary dimension d. Using effective d-dimensional collision rates ($\propto N^{1/d}$) one can convert the "one-dimensional" results in this study into a general mean-field theory.

Acknowledgments

We are grateful to K. Kornev for very fruitful remarks. This research was supported by DOE (W-7405-ENG-36).

[1] T. Harris, *The Theory of Branching Processes* (Berlin: Springer, 1963).
[2] S. K. Shrinivasan, *Stochastic Theory and Cascade Processes* (American Elsevier: New York, 1969).
[3] P. Habib, *Soil Mechanics* (Cambridge University Press: Cambridge, 1983).
[4] S. Redner, in: *Statistical Models for the Fracture of Disorder Media*, eds. H. J. Herrmann and S. Roux (North-Holland, 1990).
[5] E. W. Montroll and R. Simha, J. Chem. Phys. **8**, 721 (1940).
[6] R. Shinnar, J. Fluid Mech. **10**, 259 (1961).
[7] K. C. Chase, P. Bhattacharyya, and A. Z. Mekjian, Phys. Rev. C **57**, 822 (1998).
[8] E. D. McGrady and R. M. Ziff, Phys. Rev. Lett. **58**, 892 (1987).
[9] T. Ishii and M. Matsushita, J. Phys. Soc. Jap. **61**, 3474 (1992).
[10] L. Oddershede, P. Dimon, and J. Bohr, Phys. Rev. Lett. **71**, 3107 (1993).
[11] M. Mézard, G. Parisi, and M. Virasoro, *Spin Glass Theory and Beyond* (World Scientific, Singapore, 1987).
[12] P. G. Higgs, Phys. Rev. E **51**, 95 (1995).
[13] B. Derrida and B. Jung-Muller, J. Stat. Phys. **94**, 277 (1999).
[14] S. A. Kauffman, *The Origin of Order: Self-Organization and Selection in Evolution* (Oxford University Press, London, 1993).
[15] H. Flyvbjerg and N. J. Kjaer, J. Phys. A **21**, 1695 (1988).
[16] A. P. Siebesma, R. R. Tremblay, A. Erzan, and L. Pietronero, Physica A **156**, 613 (1989).
[17] R. C. Srivastava, J. Atmos. Sci. **39**, 1317 (1982).
[18] Z. Cheng and S. Redner, J. Phys. A **23**, 1233 (1990).
[19] M. Kostoglou and A. J. Karabelas, J. Phys. A **33**, 1221 (2000).
[20] Ph. Laurnçot and D. Wrzocek, J. Stat. Phys. **104**, 193 (2001).
[21] A. F. Filippov, Theory Phobab. Appl. **4**, 275 (1961).
[22] G. I. Barenblatt, *Scaling, Self-Similarity, and Intermediate Asymptotics* (Cambridge University Press, Cambridge, 1986)
[23] J. D. Murray, *Mathematical Biology* (Springer-Verlag, New York, 1989).
[24] M. Bramson, *Convergence of Solutions of the Kolmogorov Equation to Travelling Waves* (American Mathematical Society, Providence, R.I., 1983).
[25] W. van Saarloos, Phys. Rev. A **39**, 6367 (1989).
[26] E. Brunet and B. Derrida, Phys. Rev. E **56**, 2597 (1997).
[27] U. Ebert and W. van Saarloos, Phys. Rev. Lett. **80**, 1650 (1998); Physica D **146**, 1 (2000).
[28] E. Ben-Naim, A. R. Bishop, I. Daruke, and P. L. Krapivsky J. Phys. A **31**, 5001 (1998)
[29] S. N. Majumdar and P. L. Krapivsky, Phys. Rev. E **62**, 7735 (2000).
[30] P. L. Krapivsky and S. N. Majumdar, Phys. Rev. Lett. **85**, 5492 (2000); S. N. Majumdar and P. L. Krapivsky, Phys. Rev. E **65**, 036127 (2001).
[31] S. N. Majumdar and P. L. Krapivsky, Phys. Rev. E **63**, 045101(R) (2001).
[32] E. Ben-Naim, P. L. Krapivsky, and S. N. Majumdar, Phys. Rev. E **64**, 035101(R) (2001).
[33] The diverging density and finite mass dictate the following bounds for the exponent, $1 < \alpha < 2$.
[34] R. M. Ziff and E. M. McGrady, J. Phys. A. **18**, 3027 (1985).
[35] In deterministic fragmentation, the typical mass always decays *faster* than the average mass.